

Emission Mechanisms in X-Ray Faint Galaxies

Beth A. Brown ¹

NASA Goddard Space Flight Center, Greenbelt, MD 20771

Beth.Brown@gsfc.nasa.gov

Joel N. Bregman

Department of Astronomy, University of Michigan, Ann Arbor, MI 48109-1090

jbregman@umich.edu

ABSTRACT

Hot gas dominates the emission in X-ray luminous early-type galaxies, but in relatively X-ray faint systems, integrated X-ray emission from discrete stellar-like sources is thought to be considerable, although the amount of the contribution is controversial. To help resolve this issue, we examine the radial X-ray surface brightness distribution of 17 X-ray faint galaxies observed with the ROSAT HRI and PSPC. We assume that the stellar contribution follows a de Vaucouleurs law while the hot gas component follows a King β model. For some galaxies, both models fit equally well, but for a number of systems, a dual component model yields the best fit, from which, upper bounds are placed on the stellar contribution. Best-fit values for the stellar contribution are inconsistent with (lower than) that suggested by Fabbiano, Gioia, & Trinchieri (1989) and estimated from the bulge of M31, but are consistent with the Forman, Jones, & Tucker (1985) estimate of the stellar fraction in X-ray faint elliptical and S0 galaxies. Our results indicate an upper limit to discrete sources of $L_X/L_B = 1.6 \times 10^{29} \text{ ergs s}^{-1}/L_\odot$.

Subject headings: galaxies: elliptical and lenticular — galaxies: stellar content — galaxies: ISM — X-rays: galaxies — X-rays: ISM

¹National Research Council Fellow

1. Introduction

One key concern in the study of early-type galaxies, is the amount of discrete X-ray sources relative to hot gas in X-ray faint ellipticals. It is generally agreed that integrated X-ray emission from stellar sources (such as accreting X-ray binaries) is likely to be present at some fraction in all elliptical galaxies. This contribution is low in X-ray–luminous galaxies (i.e. $L_X/L_B \gtrsim 3.2 \times 10^{30} \text{ ergs s}^{-1}/L_\odot$), where hot, diffuse gas dominates the total X-ray emission (e.g. Forman, Jones & Tucker 1985; Canizares, Fabbiano & Trinchieri 1987; Davis & White 1996; Brown & Bregman 1998; Buote & Fabian 1998). The fraction of X-ray emission from stellar sources is expected to increase with decreasing L_X , but the L_X at which the stellar component ($L_{X,*}$) dominates the observed emission is still debated.

Using *Einstein Observatory*, *ROSAT*, and *ASCA* data, researchers have derived estimates (or upper limits) to the stellar X-ray emission in E and S0 galaxies using various methods. Forman, Jones & Tucker (1985) determined an upper limit of $L_{X,*}/L_B \simeq 4 \times 10^{28} \text{ ergs s}^{-1}/L_\odot$ (*Einstein* IPC band) by assuming discrete sources make a 50% contribution to the total diffuse X-ray emission of Cen A. In this limit, only the faintest galaxies ($M_B > -19$ in their sample) can have their X-ray emission dominated by discrete-source emission. Irwin & Sarazin (1998) concluded that the X-ray emission of faint galaxies ($L_X/L_B < 5 \times 10^{29} \text{ ergs s}^{-1}/L_\odot$) is a combination of a hard stellar component and a very soft component, which is most likely stellar in origin as well. This was inferred by comparing the X-ray “colors” of a sample of early-type galaxies to the bulge of M31 ($L_X/L_B = 3.2 \times 10^{29} \text{ ergs s}^{-1}/L_\odot$; Irwin 2000, private communication). Fabbiano, Gioia & Trinchieri (1989) used the average L_X/L_B of early-type spirals ($L_X/L_B = 4 \times 10^{29} \text{ ergs s}^{-1}/L_\odot$, for $L_X = 10^{38} - 10^{42} \text{ ergs s}^{-1}$) as the benchmark for the stellar contribution. By comparing the L_X and L_B of elliptical and S0 galaxies to spirals (in the *Einstein* 0.5–4.5 keV), they concluded that X-ray emission from hot gas is not significant in systems for which $L_X < 10^{41} \text{ ergs s}^{-1}$. In the various estimates of the stellar emission fraction, there is an order of magnitude difference, making an accurate determination even more necessary.

The primary mechanisms for the X-ray emission can be determined through the examination of X-ray spectra (e.g., Trinchieri, Kim, Fabbiano, & Canizares 1994; Loewenstein & Mushotzky 1997; Buote & Fabian 1998). A hard spectrum ($T_X \sim 10$ keV) would indicate the presence of evolved stellar sources, while soft X-rays ($T_X \sim 1$ keV) would be reflective of a hot gas component. Recent work incorporating the use of multi-temperature spectral models indicate the presence of a very soft component in addition to the hard and soft components described above, the nature of which is suspected by most to be stellar in origin but which may be due in part to a warm ISM (Pellegrini &

Fabbiano 1994; Fabbiano, Kim, & Trinchieri 1994; Kim et al. 1996). *ROSAT*, although it has better angular resolution than the *Einstein Observatory*, does not provide high enough spectral resolution to show signatures unique to a stellar population, especially in fainter systems. Another problem with spectral modeling is that acceptable fits can be obtained with both single temperature models and multi-temperature models. Even with the better resolution of *ASCA*, calibration problems at low energies may affect spectral modeling.

The use of X-ray radial surface brightness profiles offers another way to determine the relative fractions of gas and discrete sources to the observed X-ray emission. Previously, these profiles existed only for X-ray-bright galaxies for which adequate signal-to-noise data was achieved, and were used to obtain gas densities and masses, test predictions of the cooling flow model, or model the dynamical evolution of gas flows (Sarazin & White 1988; Pellegrini & Ciotti 1998; David, Forman & Jones 1991). The use of surface brightness profiles to infer the contributions to the X-ray emission has been limited, and few conclusions have been reached with regard to faint galaxies (Forman, Jones & Tucker 1985; Trinchieri, G., Fabbiano, G., & Canizares, C. R. 1986; Pellegrini & Fabbiano 1994).

Data has become available through *ROSAT* that better allow for the examination of radial surface brightness profiles of fainter galaxies. Brown & Bregman (1998, 2000) provide X-ray information on a *ROSAT* survey of early-type galaxies extending to fainter X-ray luminosities than available from *Einstein Observatory* data. In this paper, radial surface brightness profiles are used to determine or set upper limits to the stellar contribution in the less luminous galaxies of this survey.

2. The Sample

The galaxies chosen for this study (see Table 1) are the X-ray faintest galaxies of the Brown & Bregman (1998) survey of early-type galaxies. Galaxy distances are derived from Faber et al. (1989) using an $H_0 = 50$ km/s/Mpc (the McMillan et al. 1994 distance is used for NGC 5102). Values for the stellar velocity dispersion, σ , are also obtained from Faber et al. (1989), from which the dispersion temperature, T_σ , is calculated according to $kT = \mu m_p \sigma^2$ (where μ is the mean molecular weight, and σ is the one-dimensional stellar velocity dispersion). The galaxies have optical luminosities ranging from $\log(L_B/L_\odot) = 10.2\text{--}11.2$ (derived from Faber et al. 1989 magnitudes), except NGC 5102 whose distance determination indicates $\log(L_B/L_\odot) = 9.0$. X-ray-to-optical luminosity ratios fall between 5×10^{28} and $4.5 \times 10^{29} \text{ ergs s}^{-1}/L_\odot$.

The targeted galaxies are bounded by the stellar X-ray emission estimates of Forman,

Table 1:

Galaxy Properties					
Name	Dist	$\log \sigma$	T_σ	$\log L_B$	$\log \frac{L_X}{L_B}$
	Mpc	(km s $^{-1}$)	keV	(L_\odot)	($\frac{\text{ergs}^{-1}}{L_\odot}$)
N 1344	28.44 \pm 1.76	2.204	0.163	10.66 \pm 0.06	28.81 $^{+0.15}_{-0.21}$
N 1549	24.26 \pm 5.12	2.312	0.267	10.73 \pm 0.06	29.31 \pm 0.07
N 2768	30.64 \pm 6.50	2.296	0.248	10.79 \pm 0.12	29.62 \pm 0.13
N 3115	20.42 \pm 4.30	2.425	0.450	10.83 \pm 0.06	28.91 $^{+0.08}_{-0.09}$
N 3377	17.14 \pm 2.52	2.116	0.108	10.21 \pm 0.12	29.21 $^{+0.16}_{-0.19}$
N 3379	17.14 \pm 2.52	2.303	0.257	10.49 \pm 0.06	29.29 $^{+0.16}_{-0.23}$
N 3557	47.98 \pm 10.18	2.465	0.541	11.10 \pm 0.06	29.51 \pm 0.08
N 3585	23.54 \pm 4.98	2.343	0.308	10.72 \pm 0.06	29.12 $^{+0.11}_{-0.13}$
N 3607	39.82 \pm 4.84	2.394	0.390	11.18 \pm 0.12	29.64 \pm 0.12
N 4365	26.66 \pm 1.42	2.394	0.390	10.79 \pm 0.06	29.69 \pm 0.07
N 4494	13.90 \pm 2.94	2.095	0.300 ^a	10.20 \pm 0.06	29.08 $^{+0.15}_{-0.23}$
N 4621	26.66 \pm 1.42	2.381	0.367	10.78 \pm 0.06	29.01 $^{+0.14}_{-0.16}$
N 4697	15.88 \pm 3.36	2.218	0.173	10.58 \pm 0.06	29.55 \pm 0.06
N 5061	23.92 \pm 5.06	2.282	0.233	10.53 \pm 0.06	29.01 $^{+0.13}_{-0.17}$
N 5102	3.10 \pm 0.30	1.820	0.500 ^a	8.95 \pm 0.12	28.75 $^{+0.17}_{-0.21}$
N 5322	33.22 \pm 7.04	2.350	0.319	10.80 \pm 0.12	29.31 \pm 0.13
N 7507	35.00 \pm 7.42	2.377	0.361	10.82 \pm 0.06	29.31 $^{+0.20}_{-0.34}$

Columns 2, 4, & 5 derived from Faber et al. 1989 values (Distance for NGC 5102 from McMillan et al. 1994). Column 3 from Faber et al. 1989. Column 6 from Brown 1998.

^a Adopted value for T_σ .

Jones & Tucker (1985) and Fabbiano, Gioia & Trinchieri (1989). For comparison, we have converted these estimates into *ROSAT* band equivalents. The Forman, Jones & Tucker (1985) *ROSAT* equivalent is $L_{X,\star}/L_B = 3.6 \times 10^{28} \text{ ergs s}^{-1}/L_\odot$ obtained by assuming a Raymond-Smith thermal model with a Galactic N_H column density of 10^{20} cm^{-2} and $kT = 1.0 \text{ keV}$. The Fabbiano, Gioia & Trinchieri (1989) estimate is the averaged best-fit linear regression for a sample of early-type spiral galaxies. Using an average distance of 18.12 Mpc (obtained from Fabbiano, Gioia & Trinchieri's 1988 sample of early-type spiral galaxies), and spectral model parameters above, we obtain a *ROSAT* band equivalent of $L_{X,\star}/L_B = 3.6 \times 10^{29} \text{ ergs s}^{-1}/L_\odot$.

X-ray surface brightness profiles for the targeted sample were extracted out to 4–5 effective radii (r_e) from processed *ROSAT* PSPC or HRI data. Observations from both instruments exist only for NGC 1549 and NGC 5322. Details for the general data processing of these galaxies are given in Brown & Bregman (1998). A background, taken at large radius from the galaxy center (typically at $> 7r_e$), was subtracted from the data. Normalized PSPC and HRI data were blocked into $4''$ and $2''$ pixels, respectively, and subsequently binned according to the resolution of the instrument assuming azimuthal symmetry. PSPC data were binned in $25''$ wide annuli (data for NGC 3557 was binned in 35–40'' widths beyond $\sim 2r_e$ to improve signal-to-noise), and HRI data were binned in annuli of widths increasing from $5''$ to $40''$ in the outer regions where the surface brightness was lower.

Five galaxies had total surface brightness counts too low to be useful, and so were not included in further analysis. NGC 4494 and NGC 4621 were also excluded because their detections were off-axis, which affected the shape of the profiles. Of the ten remaining galaxies, eight are classified as elliptical and two as S0 galaxies (Tully 1988 classification).

3. Obtaining the Stellar Contribution

Hot, interstellar gas and discrete stellar X-ray sources are the two primary mechanisms suggested for X-ray emission in early-type galaxies. Moderate to low signal-to-noise data prevents extensive and detailed modeling, however by separately characterizing the radial surface brightness distribution due to each component, we seek to reach an initial indication of the relative fraction of stellar X-ray sources present in X-ray faint galaxies.

We use a modified King model (β model) to parameterize the X-ray emission attributable to hot gas. The β model was developed initially to describe hot gas behavior in clusters, but has been often extended to individual elliptical galaxies (Gorenstein et al. 1978; Fabricant & Gorenstein 1983; Forman, Jones & Tucker 1985; Trinchieri, Fabbiano, &

Canizares 1986). The β model takes on the form

$$S(r)_\beta = S_0 [1 + (r/r_c)^2]^{-3\beta + \frac{1}{2}},$$

where S_0 is the central brightness and r_c is the core radius of the X-ray emission. Values of $\beta \approx 0.5$ and $r_c \sim 2$ kpc are typical in brighter ellipticals where $L_X \approx 10^{39}\text{--}10^{42}$ ergs s $^{-1}$ (e.g. Sarazin 1990; Goudfrooij & de Jong 1995). X-ray emission of bright early-type galaxies, modeled with this King function, demonstrate radial surface brightness profiles that decline more slowly than optical profiles at large radii (e.g., Forman, Jones & Tucker 1985).

A de Vaucouleurs $r^{1/4}$ law is used to trace the integrated emission from discrete X-ray sources. The discrete source emission is most likely dominated by low-mass X-ray binaries (LMXBs) in the galaxy (Irwin & Sarazin 1998; David, Forman, & Jones 1991; Trinchieri & Fabbiano 1985). LMXBs come from an evolved stellar population, so their X-ray brightness distribution should follow that of stars (Pellegrini & Fabbiano 1994). A de Vaucouleurs $r^{1/4}$ law has been very successful in modeling the optical surface brightness of ellipticals (Fry et al. 1999, Burkert 1993, Hjorth & Madsen 1991), and so we adopt it here in the form

$$S(r)_* = S_e \cdot \exp\{-7.67[(r/r_e)^{0.25} - 1]\},$$

where r_e is the effective radius (the isophote radius containing half of the total luminosity) and S_e is the surface brightness at r_e . Other models, including King models, have been used to parameterize the stellar profiles of early-type galaxies. This was primarily because there is no straightforward transformation from the de Vaucouleurs function to an analytic form of the density distribution. However, since our goal is not to derive a density distribution, this is of no concern.

A fitting algorithm was developed to determine the four parameters - S_0 , r_c , β , and S_e - that best represent the data according to the models described above. The models are convolved with an instrumental point spread function (a Gaussian of 25" FWHM for the PSPC, and 5" FWHM for the HRI), which has the form

$$p(x) = \frac{1}{2\pi\sigma^2} e^{-x^2/2\sigma^2},$$

where $\sigma = \text{FWHM}/2.35$. Spherical symmetry is assumed in the convolved profiles, which take the form

$$G(r) = \frac{1}{\pi\sigma^2} \int_0^\infty \int_0^\pi e^{-x^2/2\sigma^2} g(s) d\phi x dx.$$

The function $g(s)$ is the true profile (gaseous or stellar), where

$$s^2 = r^2 + x^2 - 2x r \cos\phi.$$

Table 2:

Core Radii of Bright Elliptical Galaxies				
Name	$r_e/11$ ($''$)	β -model		
		r_c ($''$)	ν	χ^2_ν
N 1395	4.10	4.56	42	0.76
N 1404	2.43	5.68	11	2.84
N 1549	4.30	6.08	17	0.69
N 4649	6.67	7.66	30	1.49

The core radius, r_c , fitted within a β model ($\beta \sim 0.5$) and compared to HRI data using a χ^2 test. Best-fits (χ^2_ν) are for n degrees of freedom (ν).

The convolved profiles are optimized within the program by the χ^2 test, which yields the best-fit values for the four parameters. The optimization utilizes the downhill simplex method in multidimensions of Nelder & Mead (1965).

Surface brightness data for the targets were initially fitted to the β model and then the de Vaucouleurs $r^{1/4}$ law, out to 4–5 r_e . Generally, r_c was held as a fixed parameter since it often cannot be resolved by the PSPC. If adequate HRI data existed, then r_c was determined by the β model, the value of which was subsequently used in fits to the PSPC data. If useful HRI data was not available, a core radius of $r_c = r_e/10$ was adopted based upon examination of HRI data for bright elliptical galaxies (see Table 2).

Results of the β model and de Vaucouleurs $r^{1/4}$ law fits determined whether a particular profile would then be fit with a two-component function where

$$S(r)_{fit} = S(r)_\beta + S(r)_\star.$$

Theoretical calculations of β models ($\beta = 0.4, 0.5, 0.6$, and 0.7) show that where the diffuse X-ray emission can be described by $\beta = 0.5$ (common in bright ellipticals), it is not possible to conclusively distinguish between a β model and an de Vaucouleurs $r^{1/4}$ law in terms of goodness of fit (a degenerate fit, see Figure 1). A unique solution cannot be obtained with a two-component function to such a profile, therefore the $S(r)_\beta + S(r)_\star$ profile was applied only when β was determined to be steeper or flatter than ~ 0.5 .

For a dual-component fit, a best-fit parameterization to the data was first obtained. Next, upper limits to the stellar contribution (relative to the best-fit) were determined by incrementally increasing $S(r)_\star$ until the fit became unacceptable at the 90% and 98–99%

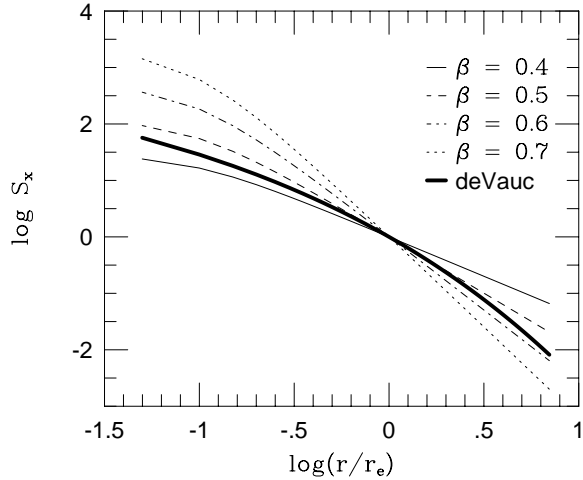


Fig. 1.— A comparison of de Vaucouleurs $r^{1/4}$ model (heavy solid curve) and β models for $\beta = 0.4$ (light solid curve), 0.5 (dashed curve), 0.6 (dotted-dashed curve), and 0.7 (dotted curve).

confidence levels:

$$\chi_{limit}^2 \approx \chi_{best}^2 + \Delta\chi^2$$

where $\Delta\chi^2 = \chi^2$ at 90% and 99% significance for 3 degrees of freedom. Once best-fit and upper limit values were found, the integrated stellar fraction was computed, from which $\log(L_{X,\star}/L_B)$ can be derived.

4. Results of the Modeling

Single component β model and de Vaucouleurs $r^{1/4}$ law model fits were performed separately to the surface brightness data for ten galaxies. A summary of the results are given in Table 3. If a galaxy had PSPC and HRI data available, fits to both data sets are summarized. In addition to r_e , fitted parameter values corresponding to the minimum χ^2 for both models are tabulated along with the number of degrees of freedom (ν) and the reduced χ^2 (χ_{ν}^2). Both β and de Vaucouleurs models fit the profiles of NGC 1549, NGC 3115, and NGC 3585 equally well (see, for example Figure 2), which is reflected in β values around 0.5. Where β was not ~ 0.5 , pure de Vaucouleurs model fits were consistently worse compared to pure β model fits, which is evidence against complete gas-depletion in these systems. Poor fits to NGC 3607 is a result of strong curvature in the brightness profile, which causes the data to be underestimated in the central region and overestimated in the

Table 3:

Single Component Galaxy Fits

Name	r_e ($''$)	β -model				$r^{1/4}$ -model			
		S_0 ($\frac{cnts}{pix}$)	r_c ^a ($''$)	β	ν	χ^2_ν	S_e ($\frac{cnts}{pix}$)	ν	χ^2_ν
N 1549(H)★	47.44	2.31	5.58	0.50	9	1.73	0.039	11	1.44
N 1549(P)★		6.38	5.58	0.46	7	3.36	0.150	8	3.12
N 2768(P)	49.44	1.44	4.94	0.41	7	0.20	0.039	8	1.75
N 3115(P)★	32.32	5.57	3.23	0.47	4	0.90	0.095	5	0.80
N 3379(H)	35.19	6.86	3.43	0.64	5	0.75	0.035	7	4.09
N 3557(P)	37.10	19.59	3.71	0.56	4	0.91	0.160	5	4.68
N 3585(P)★	38.04	1.70	3.81	0.48	5	0.79	0.027	6	0.55
N 3607(P)	65.49	4.80	6.55	0.39	11	3.03	0.150	12	17.10
N 4365(P)	56.57	4.17	5.65	0.41	8	1.84	0.110	9	6.90
N 4697(P)	73.51	9.20	7.35	0.40	12	3.53	0.260	13	22.81
N 5322(H)	34.76	2.82	3.92	0.61	6	0.77	0.023	8	1.46
N 5322(P)		19.17	3.92	0.48	4	2.94	0.340	5	1.65

Best-fits ($\chi^2_\nu = \chi^2/n$ degrees of freedom). In column 1, H=HRI, P=PSPC. A starred designation indicates both models fit equally well.

^a Core radius, r_c , fixed for PSPC data at either HRI fitted values or $r_e/10$.

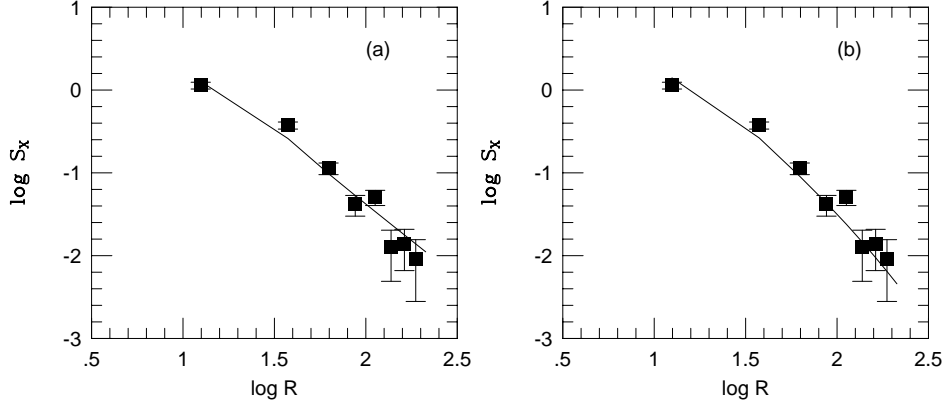


Fig. 2.— NGC 1549 PSPC data fit to β (a) and de Vaucouleurs $r^{1/4}$ (b) models. Surface brightness in cnts/pix is plotted against radius in arcsec.

outer regions. Small-scale fluctuations in the outer brightness profile of NGC 4697 also resulted in poor fits.

The results of gas-plus-stellar component models are summarized in Table 4 for the seven galaxies whose derived β values were different from 0.5 in the single-component fitting. Best-fit results as well as those for upper limits to the discrete source contribution (at the 90% and 98–99% confidence levels) are tabulated. The core radius, r_c , is fixed in all but the best-fits to HRI data. Also given in Table 4 is the integrated count fraction of the stellar component (S_*/S_{tot}), and the corresponding luminosity ratio $\log(L_{X,*}/L_B)$. In the best-fit modeling, the fraction of surface brightness counts that can be attributed to discrete sources is less than 25% for each of the seven galaxies modeled. The modeled profile of NGC 2768 (Figure 3) indicates that the stellar component is enhanced in the central regions of the galaxy versus the outer regions (relative to the gas component), the reverse of what is indicated for NGC 3557 and NGC 5322. NGC 4365 (8% stellar fraction) exhibits an approximately even ratio of stars to gas throughout the data set. The dual-component best-fits to NGC 3379, NGC 3607, and NGC 4697 are essentially the same as in single-component β modeling.

In the 90% upper limit, the stellar fraction to the combined fit ranges from around 25% to near 100%. The stellar component dominates the total emission of NGC 2768 except in the outermost regions (at $> 130''$, see Figure 4), and β flattens considerably. In NGC 3557 and NGC 5322, a steep β model curve rapidly falls at or before r_e . Here, the stellar

Table 4:

Dual Component Galaxy Fits

Name		S_0 ($\frac{cnts}{pix}$)	r_c ($''$)	β	S_e ($\frac{cnts}{pix}$)	ν	χ^2_ν ^a	$\frac{S_*}{S_{tot}}$	$\log \frac{L_{X,*}}{L_B}$ ($\frac{ergs^{-1}}{L_\odot}$)
N 2768	best	0.99	4.94	0.40	0.810E-2	6	0.23	0.16	28.83
	90%	0.24E-1	4.94	0.25	0.426E-1	6	1.28	0.79	29.52
	99%	0.19E-1	4.94	0.25	0.475E-1	6	2.12	0.84	29.54
N 3379	best	6.87	3.42	0.64	0.987E-6	4	0.94	<0.01	24.79
	90%	6.12	3.42	0.86	0.280E-1	5	1.99	0.68	29.12
	99%	5.86	3.42	0.97	0.352E-1	5	3.01	0.78	29.18
N 3557	best	18.87	3.71	0.57	0.170E-1	3	1.20	0.13	28.63
	90%	24.39	3.71	0.99	0.135	3	3.25	0.97	29.50
	99%	17.45	3.71	0.99	0.154	3	4.94	0.98	29.50
N 3607	best	4.79	6.55	0.39	0.809E-5	10	3.33	<0.01	25.16
	90%	2.27	6.55	0.36	0.583E-1	10	3.95	0.24	29.02
	99%	1.58	6.55	0.34	0.783E-1	10	4.46	0.33	29.15
N 4365	best	3.48	5.65	0.40	0.130E-1	7	2.09	0.08	28.61
	90%	0.43	5.65	0.31	0.890E-1	7	2.97	0.58	29.45
	99%	0.19	5.65	0.28	0.103	7	3.69	0.66	29.51
N 4697	best	9.22	7.35	0.40	0.123E-4	11	3.85	<0.01	25.04
	90%	4.19	7.35	0.37	0.103	11	4.41	0.27	28.97
	99%	2.88	7.35	0.35	0.136	11	4.88	0.35	29.10
N 5322	best	2.79	3.88	0.65	0.434E-2	5	0.91	0.22	28.66
	90%	1.39	3.88	0.94	0.251E-1	6	1.65	0.89	29.26
	99%	0.50E-5	3.88	0.54	0.307E-1	6	2.64	1.00	29.31

First entry for each galaxy corresponds to “best-fit.” Second and third entries for each galaxy corresponds to the 90% and 98–99% upper limits to the discrete source contribution. Core radius, r_c , is fixed for PSPC data, and fitted for best-fit to HRI data, and then fixed for subsequent upper limit fits. $\chi^2_\nu = \chi^2/n$ degrees of freedom.

^a $\chi^2_{limits} \approx \chi^2_{best} + \Delta\chi^2$, where $\Delta\chi^2 = \chi^2$ at 90% and 99% significance for 3 degrees of freedom.

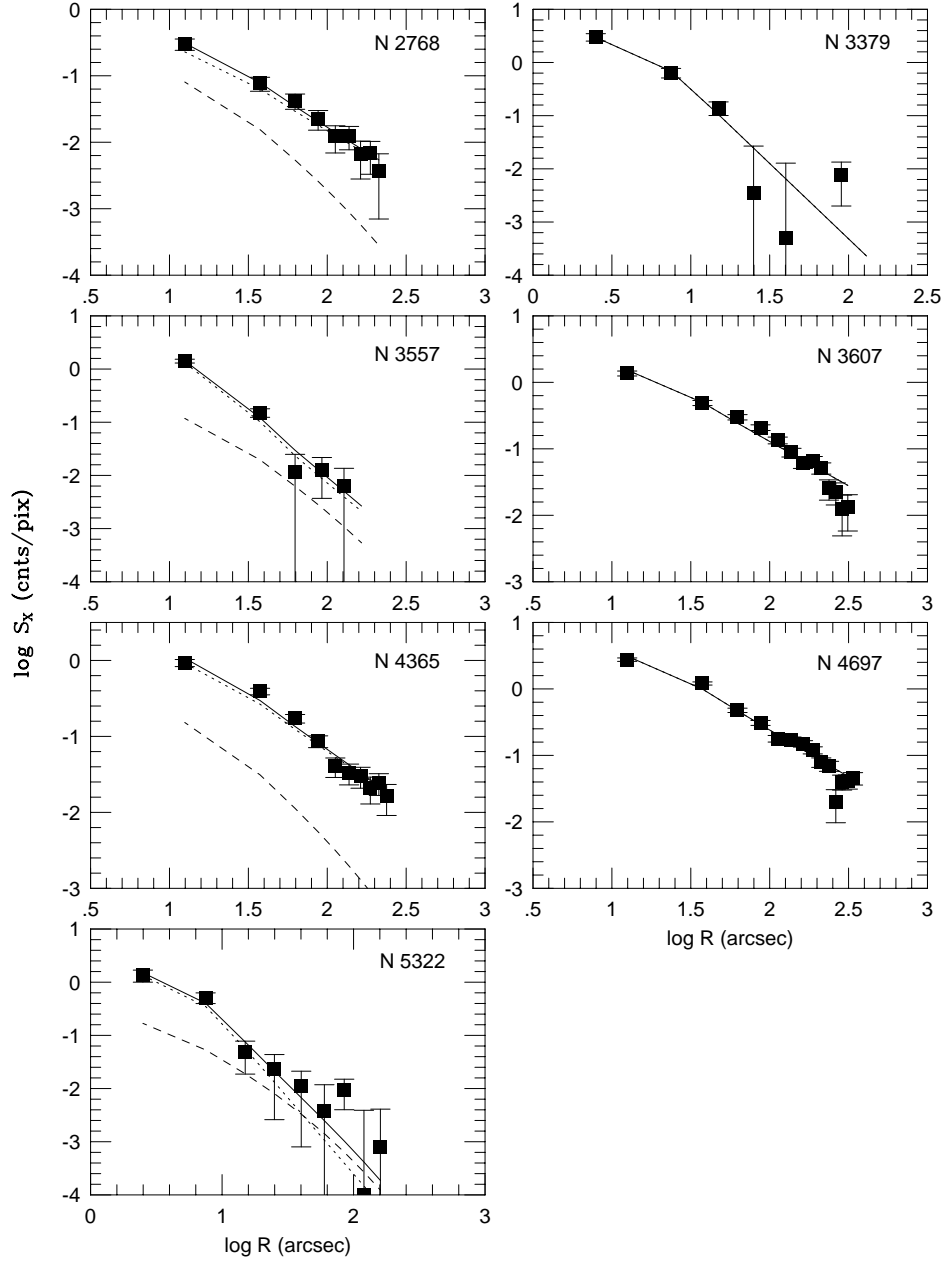


Fig. 3.— Dual-component best-fits to the profiles of NGC 2768, NGC 3379, NGC 3557, NGC 3607, NGC 4365, NGC 4697, and NGC 5322. In each plot, the dotted curve is the gas-component, the dashed curve is the stellar component, and the solid curve is the combined fit. For NGC 3379, NGC 3607, and NGC 4697 the combined fit is identical to the gas-component.

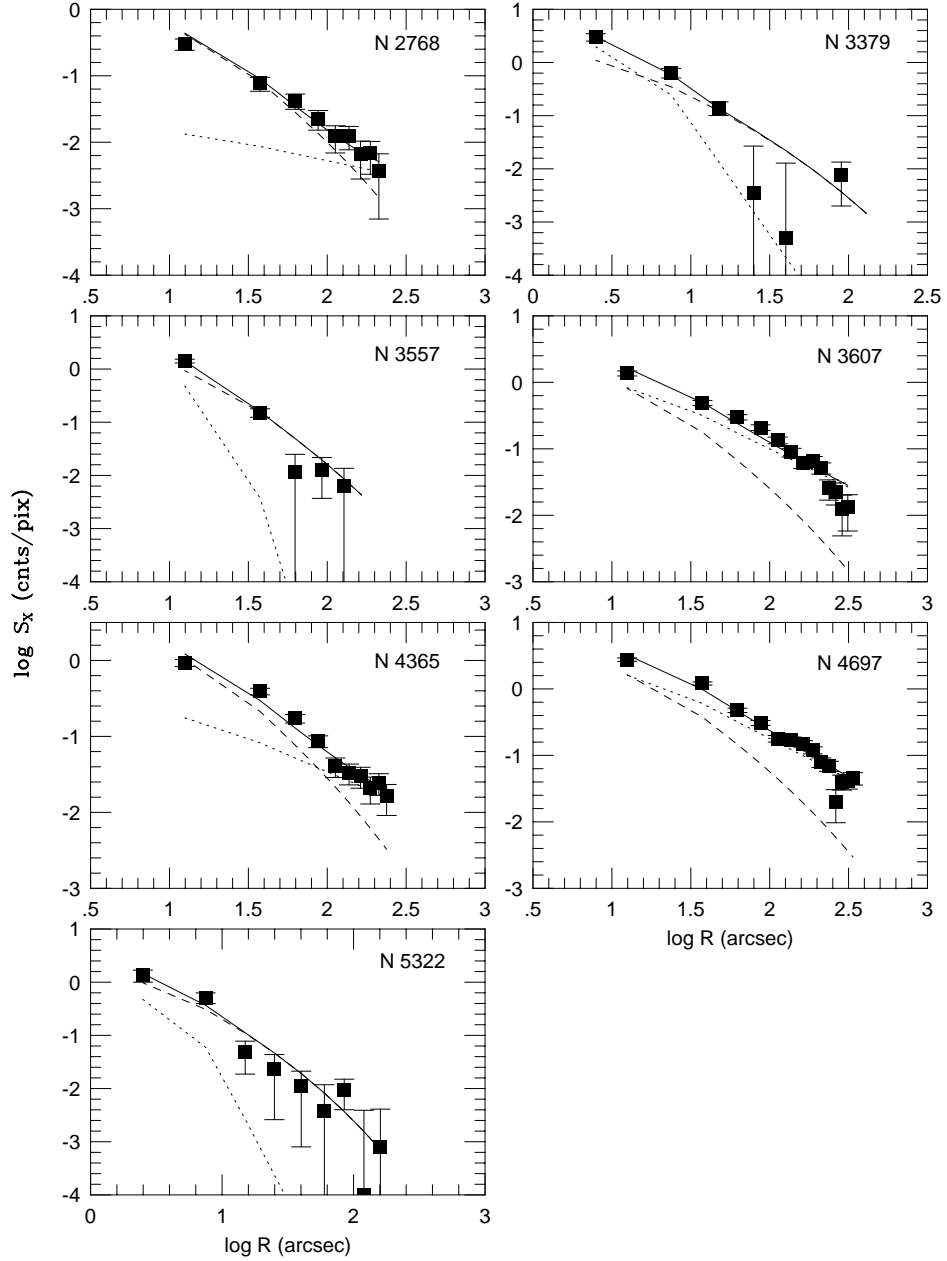


Fig. 4.— Dual-component 90% upper limit fits to the surface brightness profiles of NGC 2768, NGC 3379, NGC 3557, NGC 3607, NGC 4365, NGC 4697, and NGC 5322. Surface brightness in cnts/pix is plotted against radius in arcsec. In each plot, the dotted curve is the gas-component, the dashed curve is the stellar component, and the solid curve is the combined fit.

component dominates throughout the radial range, however gas enhancement is indicated in the center. The greatest increase in stellar fraction occurs in NGC 3379 (from <1% in the best-fit to 68%). In this galaxy, the gas component is dominant only in the very center (radius < 5''). NGC 3607 and NGC 4697 results indicate that the stellar component contributes equally, or possibly exceeds, in the very center, with gas dominating the total emission throughout the remainder of the data set. The results from NGC 4365 show stars dominating in the inner regions of the galaxy, with gas being more enhanced beyond radius $\sim 90''$.

5. Discussion

We compare the modeled estimates of the stellar fraction to the estimates of Forman, Jones & Tucker (1985, FJT) and Fabbiano, Gioia & Trinchieri (1989, FGT), and that estimated from M31 (Irwin 2000, private communication). The linear curves are superimposed upon a plot of the X-ray luminosities of the targeted galaxies against their optical blue luminosities (Figure 5). For $\log(L_B/L_\odot) = 10.4 - 11$, the total L_X of our sample spans the region between these estimates. The seven galaxies, whose radial surface brightness profiles could be fitted with combined King and de Vaucouleurs models, all have total L_X/L_B values in the brighter half of the region of interest. The best fit and 90% upper limit $L_{X,*}$ values are plotted for those galaxies as well.

Best-fit modeling indicates a hot gas-dominated emission in each of the seven galaxies fit with the combined profile. The median for the best fits is $\log(L_{X,*}/L_B) = 28.61$ (L_X in ergs s^{-1} and L_B in L_\odot), in reasonable agreement with the Forman, Jones & Tucker (1985) upper limit of $\log(L_{X,*}/L_B) = 28.6$. In the 90-99% upper limit, however, all but two of the seven galaxies can be modeled with a combination profile indicative of a stellar-dominated emission. The median for the 99% confidence fits is $\log(L_{X,*}/L_B) = 29.31$, which is a factor of ~ 1.8 and 1.6 below the limits of Fabbiano, Gioia & Trinchieri (1989) and M31 respectively. We further find 3σ upper limits of $\log(L_{X,*}/L_B) = 29.15 - 29.26$ for the X-ray faintest galaxies not modeled, assuming that all of the observed emission is stellar. We suggest, then, an upper limit to $\log(L_{X,*}/L_B)$ of 29.2 for the integrated X-ray emission from discrete sources in X-ray faint early-type galaxies. This supports the Irwin & Sarazin (1998) suggestion that the brightest of X-ray faint galaxies ($\log L_{X,*}/L_B < 29.7$) may retain a significant amount of gas with a temperature of 0.3–0.6 keV.

We explore how our results may relate to recent spectral studies of faint E and S0 galaxies. *ASCA* studies of early-type galaxies confirm a hard spectral component attributed to the integrated emission from LMXBs (e.g., Matsumoto et al. 1997), and a very soft

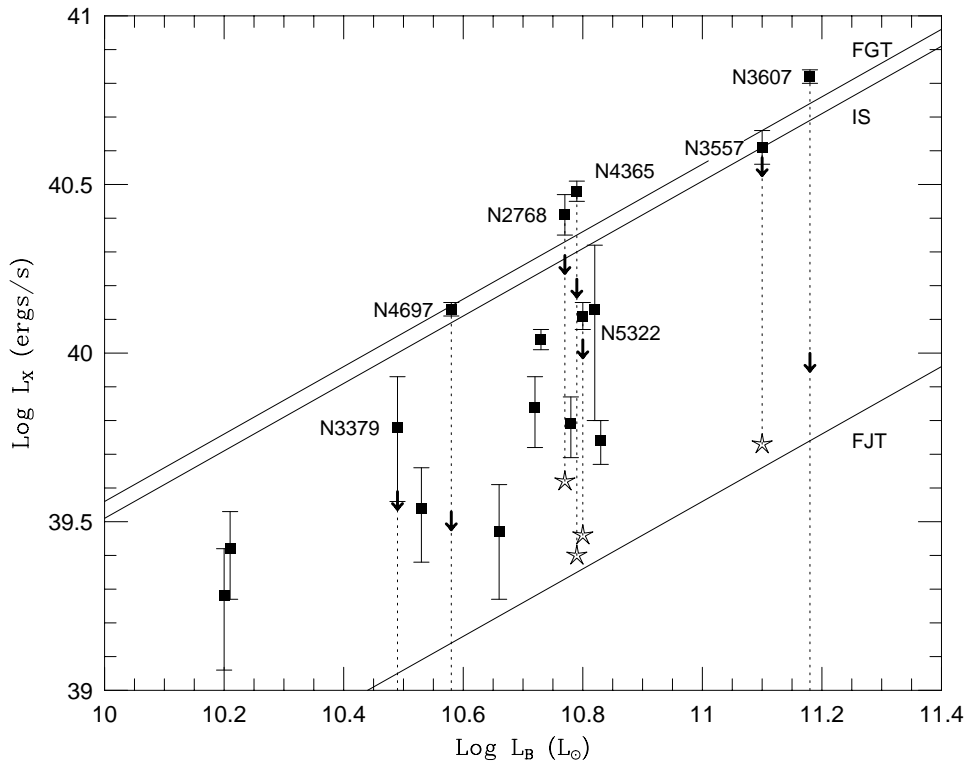


Fig. 5.— X-ray vs. optical luminosities for the target sample. Errors in L_X are due to photon statistics. L_B for NGC 2768 has been artificially lowered by 0.02 in the log for clarity, and NGC 5102 lies beyond the plot boundaries. Stars are the “best-fit” $L_{X,*}$ values determined from a two-component fit while downward arrows are 90% upper limits. The linear lines are the stellar estimates of Forman, Jones & Tucker (1985, FJT) and Fabbiano, Gioia & Trinchieri (1989, FGT), and estimated from M31 (Irwin 2000, private communication) with $\log(L_{X,*}/L_B) = 28.56$, 29.56 , and 29.51 respectively ($L_{X,*}$ in ergs s^{-1} , L_B in L_\odot).

component (VSC), initially detected in *ROSAT* data (Kim, Fabbiano, & Trinchieri 1992; Kim et al. 1996). For galaxies with $\log L_X/L_B \geq 30.0$, spectral signatures harden as L_X/L_B decreases, until the hard component dominates the emission. The Kim et al. (1996) study of an X-ray faint S0 galaxy, NGC 4382, reports that the hard spectral component contributes one-half to three-fourths of the total X-ray luminosity, with the remainder due to the VSC. This is consistent with the earlier *ROSAT* results which indicate that the VCS and hard components contribute near equally to the total X-ray emission in galaxies with $\log L_X/L_B \leq 30.0$ (L_X in ergs s⁻¹ and L_B in L_\odot). The VSC may be due to a warm ISM, arise from stellar sources, or be a combination of both (Irwin & Sarazin 1998; Fabbiano, Kim, & Trinchieri 1994). Our results may be indicative of the VSC having an ISM origin, considering that the best-fit modeling is consistent with a substantial ISM component.

In this initial analysis of X-ray surface brightness profiles, we have assumed low-mass X-ray binaries (LMXBs) are the primary constituents of a discrete X-ray source population. LMXBs contribute to the bulk of X-ray emission in large spiral bulges such as M31 (Trinchieri & Fabbiano 1985). Because spiral bulges are very similar to elliptical galaxies in their properties and stellar populations, it is reasonable to presuppose that LMXBs are also the main contributors to the discrete source population in early-type galaxies (David, Forman, & Jones 1991; Irwin & Sarazin 1998). However, it is possible that globular clusters may be a significant source of X-ray emission in X-ray faint E and S0 galaxies (Trinchieri & Fabbiano 1985), in which case the X-ray radial brightness distribution due to non-gaseous sources may be more appropriately described by a model other than a pure de Vaucouleurs $r^{1/4}$ law.

The goal of finding the stellar contribution in X-ray faint galaxies has been hampered by low photon counts and lack of data from both *ROSAT* detectors. Long observations with Chandra will be especially helpful in constraining the core radii in faint galaxies, fixing the shape of the radial surface brightness profiles, and resolving bright point sources. It is also hoped that Chandra will provide the spectral resolution needed to determine whether the “very soft component” modeled by various authors (see §1) is due to a warm ISM of to discrete sources. Additionally, techniques that circumvent the problem of low counts, such as defining X-ray “colors” (Irwin & Sarazin 1998), will be helpful in obtaining a definite answer to the long-standing question of dominant emission mechanisms in X-ray faint early-type galaxies.

We would like to thank J. Irwin and J. S. Arabadjis for valuable discussion, and the anonymous referee for helpful comments. Also, we wish to acknowledge the use of the NASA Extragalactic Database (NED), operated by IPAC under contract with NASA. B. Brown would like to acknowledge support through a NASA Graduate Student Researchers

Program grant NGT-51408 and a National Academy of Science research associateship NRC-9822890. J. Bregman acknowledges NASA grant NAG5-3247.

REFERENCES

- Brown, B. A. 1998, Ph.D. Thesis, University of Michigan.
- Brown, B. A., & Bregman, J. N. 1998, ApJ, **495**, L75, astro-ph/9712209.
- Brown, B. A., & Bregman, J. N. 2000, ApJ, **539**, 592.
- Buote, D. A., & Fabian, A. C. 1998, MNRAS, **296**, 977, astro-ph/9707117.
- Burkert, A. 1993, A&A, **278**, 23.
- Canizares, C. R., Fabbiano, G., & Trinchieri, G. 1987, ApJ, **312**, 503.
- David, L. P., Forman, W. & Jones, C. 1991, ApJ, 369, 121.
- Davis, D. S., & White, R. E. 1996, ApJ, 470, L35, astro-ph/9607052.
- Fabbiano, G., Gioia, I. M., & Trinchieri, G. 1988, ApJ, **324**, 749.
- Fabbiano, G., Gioia, I. M., & Trinchieri, G. 1989, ApJ, **347**, 127.
- Fabbiano, G., Kim, D.-W., & Trinchieri, G. 1994, ApJ, **429**, 94.
- Faber, S. M., Wegner, G., Burstein, D., Davies, R. L., Dressler, A., Lynden-Bell, D., & Terlevich, R. J. 1989, ApJS, 69, 763.
- Fabricant, D., & Gorenstein, P. 1983, ApJ, **267**, 535.
- Forman, W., Jones, C., & Tucker, W. 1985, ApJ, **293**, 102.
- Fry, A. M., Morrison, H. L., Harding, P., Boroson, T. 1999, in The Third Stromlo Symposium: The Galactic Halo, eds. Gibson, B.K., Axelrod, T.S. & Putman, M.E., ASP Conference Series, **165**, 197.
- Gorenstein, P., Fabricant, D., Topka, K., Harnden, F. R., Jr., & Tucker, W. H. 1978, ApJ, **224**, 718.
- Goudfrooij, P. & de Jong, T. 1995, A&A, **298**, 784, astro-ph/9504011.
- Hjorth, J., Madsen, J. 1991, MNRAS, **253**, 703.
- Irwin, J. A., & Sarazin, C. L. 1998, ApJ, **499**, 650, astro-ph/9804210.
- Kim, D.-W., Fabbiano, G., Matsumoto, H., Koyama, K., & Trinchieri, G. 1996, ApJ, **468**, 175.
- Kim, D.-W., Fabbiano, G., & Trinchieri, G. 1992, ApJ, **393**, 134.
- Loewenstein, M. & Mushotzky, R. F. 1997, *Proceedings of IAU Symposium 187 on Cosmic Chemical Evolution*, astro-ph/9710339.

- Matsumoto, H., Koyama, K., Awaki, H., Tsuru, T., Loewenstein, M., Matsushita, K. 1997, ApJ, **482**, 133, astro-ph/9701077.
- McMillan, R., Ciardullo, R., & Jacoby, G. H. 1994, AJ, 108, 1610.
- Mihalas, D., & Binney, J. 1981, *Galactic Astronomy* (New York: W. H. Freeman and Company).
- Nelder, J. A. & Mead, R. 1965, *Computer Journal*, **7**, 308.
- Pellegrini, S. & Ciotti, L. 1998, A&A, **333**, 433, astro-ph/9802035.
- Pellegrini, S. & Fabbiano, G. 1994, ApJ, **429**, 105, astro-ph/9312046.
- Sarazin, C. L. 1990, in The Interstellar Medium in Galaxies, eds. H. A. Thronson, Jr. & J. M. Shull (Dordrecht: Kluwer), 201.
- Sarazin, C. L & White, R. III 1988, ApJ, **331**, 102.
- Trinchieri, G., & Fabbiano, G. 1985, ApJ, **296**, 447.
- Trinchieri, G., Fabbiano, G., & Canizares, C. R. 1986, ApJ, **310**, 637.
- Trinchieri, G., Kim, D.-W., Fabbiano, G., & Canizares, C. R. C. 1994, ApJ, **428**, 555.
- Tully, R. B. 1988, *Nearby Galaxies Catalog* (Cambridge University: Cambridge)